Journal of Magnetic Resonance 272 (2016) 100–107

Contents lists available at ScienceDirect

Journal of Magnetic Resonance

journal homepage: www.elsevier.com/locate/jmr

Usage of internal magnetic fields to study the early hydration process of cement paste by MGSE method

Janez Stepišnik [a,b,*], Ioan Ardelean [c]

[a] University of Ljubljana, Faculty of Mathematics and Physics, Physics Department, Jadranska 19, 1000 Ljubljana, Slovenia
[b] Institute Jožef Stefan, Jamova 39, 1000 Ljubljana, Slovenia
[c] Physics Department, Faculty of Materials Science and Engineering, Technical University of Cluj-Napoca, Romania

ARTICLE INFO

Article history:
Received 15 July 2016
Revised 16 September 2016
Accepted 17 September 2016
Available online 17 September 2016

Keywords:
Magnetic resonance
Structure of porous media
Diffusion
CPMG
Modulated gradient spin echo
Velocity correlation function
Cement
Hydration process
Magnetic susceptibility

ABSTRACT

Internal magnetic field gradients, arising within the porous media due to susceptibility differences at the interfaces of solid and liquid as well as due to the contained magnetic impurities, can be employed by the method of modulated gradient spin echo to get insight into the velocity autocorrelation spectrum of liquid confined in the porous structure. New theoretical treatment of spin interaction with the radio-frequency field and the simultaneously applied static non-uniform magnetic field provides the formula that match well with the measurement of restricted diffusion of water in pores of cement paste. Its fitting to the experimental data gives the changes in the mean size of capillary pores, the spin relaxation and the magnitude of mean internal magnetic field gradients during the induction period and early acceleration stage of hydration processes at different temperatures.

1. Introduction

The cement paste is a material with a complex porous structure containing pores ranging from nanometers to micrometers and represents the main constituent of all cement based materials (concrete, mortars) [1,2]. The cement paste is obtained by the hydration of Portland cement grains in the presence of water [1]. The material resulting from the hydration reaction is a rigid and complex mixture of various minerals, both highly crystalline, such as ettringite and Portlandite, as well as minerals with a weak crystalline structure, namely C—S—H (here we use the cement chemistry abbreviations) [1]. The C—S—H is a heterogeneous nano-porous material containing sheets of calcium, oxygen atoms and silicate tetrahedra separated by sheets of water [3,4]. Along with the remaining non hydrated cement grains and the admixtures, the growth of these minerals creates inside the cement based materials a porous network in which three pore types can be distinguished: intra-C—S—H sheet pores, inter-C—S—H gel pores and capillary pores [3].

The hydration reaction is influenced by a variety of internal and external factors such as the presence of different admixtures (silica fume, fly ash) [1,5] or additives (superplasticizers, silanes) [6–8] as well as by the curing temperature [9]. These factors influence both the pore size and their connectivity, with important consequences on the final strength and durability of cement based materials (concrete, mortars). It is already known that capillary pores allow the penetration of carbon dioxide and of sulfate in various forms, leading to carbonation, as well as cracking, spalling and general loss of durability due to external sulfate attack [10]. That is why, decreasing the permeability of the cement based materials used in general applications allows for an increase in long-term durability, protection of steel reinforcements and reduction of deterioration, by preventing the ingress of highly reactive chemicals from the environment. To control the permeability, reliable methods for pore size determination are mandatory. These methods should allow monitoring of the pore size evolution even during the hydration process.

The NMR relaxometry techniques allow in principle the pore size determination even during sample evolution provided that the relaxivity constant is known [2,11]. One option would be to calculate the relaxivity constant by taking into account the magnetic impurity content of the cement sample [2]. This approach is

* Corresponding author at: University of Ljubljana, Faculty of Mathematics and Physics, Physics Department, Jadranska 19, 1000 Ljubljana, Slovenia.
E-mail address: Janez.Stepisnik@fmf.uni-lj.si (J. Stepišnik).

http://dx.doi.org/10.1016/j.jmr.2016.09.013
1090-7807/

however cumbersome and relies on the assumption that the only relaxation mechanism in cement based materials is determined by the interaction of the proton spins with the paramagnetic centers located on the pore surface [12]. The other option for the relaxivity calibration would be to compare the relaxation data with the pore sizes provided by different techniques. Note however that this task is difficult to be accomplished in the case of cement paste due to the fact that the pore surface continuously changes during the hydration process [9]. Moreover, it has been already shown that even for the hardened cement-based materials the mercury porosimetry technique is an inappropriate method for the measurement of pore size distributions [13]. Furthermore, different techniques may lead to pore dimensions differing by orders of magnitude [14]. Consequently, an alternative approach which does not require the knowledge of the relaxivity constant should be implemented in systems with pore evolution.

A widely used NMR approach for determining the pore sizes of porous media without the need for previous calibrations of the relaxivity constant relies on time dependent diffusion measurements [15]. The most implemented technique for diffusion measurements in porous media uses the pulsed magnetic field gradient (MFG) stimulated echo sequence [15]. The main drawback of this sequence is however that it is restricted to the porous samples with low internal gradients [16]. The internal MFG are generated inside pores due to the susceptibility differences between the porous matrix and the confined liquid [17]. They are proportional with the external magnetic field and are enhanced by the presence of magnetic impurities in the cement grains or in other components of the cement mixture. These MFG which overlap the external gradient used for diffusion measurements make the diffusion measurements unreliable. A solution to overcome this problem is to use compensating pulse sequences [16]. Note however that implementing of compensating pulse sequences requires the rapid switching of MFG pulses and this is problematic for investigation of water inside cement samples, due to the short transverse relaxation time.

Previous investigations have shown that the internal MFG may have not only a negative role in NMR diffusion measurements but they can be also exploited as an instrument for the pore size characterization [18–20]. One such approach takes into consideration the influence of internal MFG of the echo train arising in a Carr-Purcell-Meiboom-Gill (CPMG) experiment [18,20,21]. On this basis, it was possible to extract information about the pore size evolution of cement paste without the need of previous calibration for the relaxivity constant [21]. Note however that the interpretation of the CPMG echo decays in the frame of the theory derived in Ref. [18] by adapting the scattering theory from quantum mechanics is strictly valid for short diffusion times when diffusion length is much smaller both than the structural length of the sample and the dephasing length defined by the distance a tagged molecule must diffuse in order to dephase by radians. This limiting condition could introduce errors in the evaluation of the data and make the technique more appropriate for bigger pores.

To overcome the above mentioned limitation, in the present work the modulated gradient spin echo (MGSE) approach [22] will be used to get insight into the velocity autocorrelation spectrum of liquid molecules confined inside the porous structure. For that purpose, a new theoretical formalism of spin interactions with the radio-frequency field and the simultaneously applied internal magnetic field was developed. The formula for the relaxation attenuation of the CPMG echo train will be compared with the experimental data on cement paste during early hydration. This will allow estimation of the changes taking place in the mean size of capillary pores and the magnitude of the mean internal MFG during the hydration process at two different curing temperatures.

2. Internally induced magnetic field gradient and the MGSE method

Using the conventional NMR technique, the externally applied MFG is superimposed to the internally generated fields, which makes the diffusion measurements very cumbersome [17]. Moreover, the measurements with PGSE method are limited in the ability to measure short diffusion times and thus limited with the size of pores, which can be probed in the porous medium. Here, we are concern with the NMR method, termed the modulated gradient spin echo (MGSE) [23], which allows a direct insight into the molecular velocity autocorrelation spectrum. In fact, it is the CPMG sequence of π-radiofrequency (RF) pulses [24,25] combined with MFG [26,27]. The CPMG sequence was initially introduced to provide reliable measurements of T_2, because a large number of RF pulses applied in short enough intervals, τ, suppresses the attenuation created by the molecular self-diffusion attenuation in the non-uniform magnetic fields [24,25]. Much later, another property of the CPMG sequence was discovered: When applied simultaneously with MFG, it does not remove unwanted effect of diffusion but on the contrary, it reveals the details of diffusion processes, which are hidden in the velocity autocorrelation spectrum (VAS) of the diffusion motion. The velocity autocorrelation function is the key quantity of the dynamic molecular system that contains details about the underlying nature of molecular interactions. In the case of restricted diffusion the VAS holds also information about the structure of porous media.

When using the version of MGSE, which combines the CPMG train with the pulses of MFG [27], the upper limit to the sampling frequency is determined by the rate of MFG pulses, which is limited by the gradient coil induction. The method allowed the studies of flow through porous media [27], the restricted diffusion in porous media [22,28–30] and the diffusion in emulsions [29], Because the maximal achievable frequency was below 1 kHz, this method prevents the study of restricted diffusion in pores smaller than a few μm. No such upper limit applies to the method combining CPMG with the fixed MFG. This version of MGSE was proposed for the first time in reference [23], but with a concern about the side effects introduced by the application of RF pulses in the presence of a background inhomogeneous magnetic field [23,31,32]. Therefore, in the first part of the article we are revealing some new understanding of spin dynamics in the case of simultaneous application of RF-pulses and inhomogeneous magnetic field. The rest of article is dedicated to the use of this method for the study of restricted water dynamics in the matrix of hydrating cement.

2.1. Spin dynamics

In the quantum mechanical notation, the interaction of the spin system with RF field and the magnetic fields, which consist of the uniform static external magnetic field applied along longitudinal z-axis, B_{oz}, and the additional non-uniform magnetic field $\vec{B}(\vec{r})$ internally induced by the susceptibility differences or/and magnetic impurities, is described by the Hamiltonian

$$\mathcal{H} = -\hbar\sum_i [\omega_o \mathcal{I}_{zi} + \vec{\omega}(\vec{r}_i)\vec{\mathcal{I}}_i] + \mathcal{H}_{rf}(t) + \mathcal{H}_{sL}, \quad (1)$$

in which the sum is taken over all individual spins and where $\vec{\omega}(\vec{r}_i) = \gamma\vec{B}(\vec{r}_i)$ denotes the resonance off-set frequency of the i-th spin at location $\vec{r}_i$. The CPMG sequence, which begins with $\pi/2$-RF pulse to turn magnetization from the longitudinal into the transverse direction along y-axis, is followed by the train of π pulses with the RF magnetic field applied along y-axis. It is described by $\mathcal{H}_{rf}(t) = \mathcal{H}^x_{\pi/2}(t) + \mathcal{H}^y_{cpmg}(t)$ in which the spin manipulation with the train of π-RF pulses is included in $\mathcal{H}_{cpmg}(t) = -2\hbar\omega_\pi(t)$

$\cos(\omega_o t)\sum_i \mathcal{I}_{yi}$. $\mathcal{H}_{sL}$ is the spin interactions with the surroundings that can be divided into the part concerning the spin relaxation, $\mathcal{H}_{rL}$, responsible for T_1 and T_2, but unconnected to the translational motion, and into the term $\mathcal{H}_{tL}$ concerning the processes of particle migrations. In the first part of our consideration we will focus only to the particle transversal displacements, while the relaxation decay will be included at the end.

The dynamics of the system is given by the density matrix

$$\rho(t) = \mathcal{U}(t)\rho(0)\mathcal{U}^{-1}(t), \tag{2}$$

in which the operator $\mathcal{U}(t)$ sets time-line. In the high temperature approximation, the initial state $\rho(0) = \beta\sum_i \mathcal{I}_{zi}$ is given by thermodynamic equilibrium in the external magnetic field, when $B_{oz} \gg |\overrightarrow{B_{gi}}|$. The formal relation between the evolution operator and the Hamiltonian (Eq. (1)) is

$$\mathcal{U}(t) = \mathcal{T}\, \mathrm{e}^{-\frac{i}{\hbar}\int_0^t \mathcal{H}(t')\,dt'}, \tag{3}$$

in which the operator $\mathcal{T}$ implies time ordering of interaction. By knowing the time evolution operator, the expectation value of physical quantity A, described by the operator $\mathcal{A}$, is given by $\langle A\rangle = Tr[\mathcal{A}\rho(t)]$.

However, the density matrix formalism becomes very cumbersome when applied to a system of spins, under the influence of a complex pulse sequence and fields. A ways of dealing with such system dynamics is by using Feynman's operator calculus [33,34], in which the transformation into the interaction representations disentangle the evolution operator into the product of time variation, rotation and tilting operators [26,23]

$$\mathcal{U} = \mathcal{U}_L\mathcal{U}_o\mathcal{U}_{gt}\mathcal{U}^y_{cpmg}\mathcal{U}^x_{\pi/2} \tag{4}$$

In the first step of the above procedure, we separate $\mathcal{U}_L$ with the Hamiltonian $\mathcal{H}_{tL}$, in order to transform the spin location into the frame giving the time dependence to $\overrightarrow{r}_i(t)$. The subsequent cessation of $\mathcal{U}_o$, which describes the spin precession in the main magnetic field, transforms the spin system into the frame rotating with ω_o. In this frame, we can neglect the terms of transformed Hamiltonian, which oscillate with ω_o or $2\omega_o$, if $\omega_o \gg \overrightarrow{\omega}(t, \overrightarrow{r}_i), \omega_\pi$. Thus, only remaining term is the component of $\overrightarrow{\omega}(t, \overrightarrow{r}_i)$ pointing along the main field, i.e. $\omega_z(t, \overrightarrow{r}_i)$, and the non-oscillating component of $\mathcal{H}^y_{cpmg}$. In the final disentanglement of $\mathcal{U}^y_{cpmg}$, the spin system is transformed into the tumbling frame, in which $\omega_z(t, \overrightarrow{r}_i)\mathcal{I}_{zi}$ changes the sign according to the repetition and the duration of π-RF pulses [26]. After all above transformations the dynamics of spins is described by the evolution operator $\mathcal{U}_{gt}(t)$ with the Hamiltonian

$$\mathcal{H}_{gt}(t) = -\hbar\sum_i \omega_z(\overrightarrow{r}_i(t))[\mathcal{I}_{zi}\cos b(t) - \mathcal{I}_{xi}\sin b(t)]. \tag{5}$$

In the transformation into the tumbling frame, $\mathcal{U}^y_{cpmg}$ is placed in front of $\mathcal{U}_{gt}$ in order to surrender the mismatch of RF pulses in background of nonuniform magnetic field, to the Hamiltonian in Eq. (5) and, in addition, that the dynamics of $\mathcal{I}_{yi}$-component of magnetization is not governed by $\mathcal{U}^y_{cpmg}$, but only by $\mathcal{U}_L\mathcal{U}_o\mathcal{U}_{gt}$, when π-RF pulses are well adjusted. Thus, Eq. (5) includes the effects of molecular motion in $\overrightarrow{r}_i(t))$, while the resonance off-set distortions are described by its second term. The time dependence of the first term of Eq. (5) with $\cos b(t)$, in which $b(t) = \int_0^t \omega_\pi(t')dt'$, tumbles between ± 1 giving an appearance of $\omega_z(t, \overrightarrow{r}_i(t))$ turnaround after each π-RF pulse. In the approximation of infinitely short π-RF pulses, the fast transition between $\pm$-states permits to neglect the effects of the second term. However, it does not hold for arbitrary narrow π-RF pulses, when the short pulses along $\mathcal{I}_x$ appear in the interval of transition, δ. These pulses bring about an additional spin rotation, which results into the resonance off-set distortions, which could spoil the measurement of molecular self-diffusion by the MGSE method.

Dynamics of such system is commonly treated by the iterations procedure of many consecutive spin rotations by which the overall evolution between the initial condition and the end of the N-th cycle is provided [35]. Another approach is by the method of "coherence pathways", which is limited to a small number of RF-pulses [36–38]. However, the last method introduces a misconception that only a "direct coherence pathway" provides a properly shaped effective MFG to be used for the MGSE method. In the attempt to get rid of unwanted pathways, the authors of Ref. [39] used the analysis with the Fourier transformation of echo signals from the time into the frequency domain claiming that only zero frequency component of echo spectrum gives a proper information about the molecular motion. This is contrary to the basic principle of diffusion measurement by the gradient spin echo, by which only the attenuation of spin echo peak conveys information about molecular translational motions [40,26,23]. The Fourier transformation of echo gives the image of spin spatial distribution, while the peak of spin echo signal, which is by definition the integral over the echo spectrum, $E(N\tau) = \int E(\omega)d\omega$, does not includes information about spin location, but only about the spin transversal motion. This is similar to the uncertainty principle in the quantum mechanics: "More precisely the position of a particle is given, the less precisely can one say what its momentum is." Thus, the analysis introduced in Ref. [39] gives a distorted information about the velocity autocorrelation spectrum.

A better approach is with the Magnus expansion of the time evolution operator, $\mathcal{U}_g(t)$ [41], which expansion to the third order of cumulant series shows that the first term of Eq. (5) provides information about spin motion hidden in the peak amplitude of spin echoes, while its second term describes the resonance offset distortion. The calculation of the resonance offset effect [42,43] gives the reduction of the echo amplitude for the factor $\frac{2}{\Delta\phi}\arctan\Delta\phi/2$ with $\phi = \frac{\delta}{\pi}\gamma|\nabla B_{zg}\Delta\overrightarrow{r}|$ and adds a small undulation to the echo decay with the frequency and the amplitude proportional to $|\Delta\overrightarrow{r}|$, which is the size of excited part the sample. In the case of the externally applied fixed MFG, $|\Delta\overrightarrow{r}|$ is determined by the initial selective excitation with the $\pi/2$-RF pulse, while for the diffusion in porous matrix, the internal susceptibility induced MFG determines the width of excitation area. This calculation shows the resonance off-set as the reduction in echo amplitudes to which a small periodic oscillation is added. Thus, the average over echo oscillation gives the decay of spin echoes that conveys a reliable information about molecular diffusion even in the case of measurement in the background of very strong inhomogeneous magnetic field of one-sided magnets [44].

Hereafter, we are focusing to the spin echo peaks containing information about the molecular motion, but taking into account the above mentioned resonance off-set effects at the signal analysis.

2.2. MGSE measurement of velocity autocorrelation spectrum

Assuming the uniform sensitivity of the receiver coil across the excited volume of sample, the evolution of the density matrix $\rho(t)$ gives the e.m.f. signal induced by y-component of magnetization [45]

$$E(t) = \hbar\gamma\frac{d}{dt}\sum_i Tr\,\rho(t)\mathcal{I}_{yi} \approx \sum_i \langle \mathrm{e}^{i\int_0^t \omega_z(\overrightarrow{r}_i(t'))\cos b(t')dt'}\rangle. \tag{6}$$

The periodicity and the zero values of the function $f(t) = \int_0^t \cos(b(t))dt$, permits to write at the peak echo amplitude at the points $t = N\tau$ as

$$E(t) = \sum_i \left\langle e^{-i\int_0^t \nabla\omega_z(\vec{r}_i(t')).\vec{v}_i(t')f(t')dt'} \right\rangle. \quad (7)$$

which shows that the velocity of i-th spin $\vec{v}_i$ is encoded in the echo peak amplitude and where $\langle \ldots \rangle$ is the time average over the particle migration in the time interval of sequence application. With the assumption that the velocity fluctuations, $\Delta\vec{v}_i(t) = \vec{v}_i(t) - \langle \vec{v}_i(t) \rangle$ behaves as a random variable, the expansion of Eq. (7) into the cumulant series to the second order (Gaussian approximation) transforms the time average of the signal into the averages of its phase as [26]

$$E(t) = \sum_i E_{oi} e^{i\alpha_i(t)-\beta_i(t)}. \quad (8)$$

The tumbling of $f(t)$ between ± 1 averages out $\alpha_i(t) = \int_0^t \nabla\omega_z(\vec{r}_i(t')).\langle \vec{v}_i(t') \rangle f(t')dt'$ in the time of a few CPMG cycles, although $\langle \vec{v}_i(t') \rangle$ may not be zero within the pore volume [46], while the transformation from the time to the frequency domain gives the echo attenuation [23]

$$\beta_i(t) = \frac{1}{\pi}\int_0^\infty \vec{q}_i(\omega,t)\underline{D}_i(\omega)\vec{q}_i(\omega,t)^* d\omega. \quad (9)$$

in which the tensor of VAS is

$$\underline{D}_i(\omega) = \int_0^\infty \langle \Delta\vec{v}_i(t) \otimes \Delta\vec{v}_i(0) \rangle e^{i\omega t} dt. \quad (10)$$

with $\otimes$ denoting the tensor product and with $\vec{q}(\omega,t) = \nabla\omega_z(\vec{r}_i)f(\omega,t)$ [26,47] being the spectrum of the spin phase discord determined by the spectrum of $f(t)$. After, a few CPMG cycles, $(N > 4)$ [27], the power spectrum of $f(t)$ can be approximated

$$|f(\omega,t)|^2 \approx 2\pi t \sum_{k=-\infty}^{\infty} |c_k|^2 \delta(\omega - k\omega_m), \quad (11)$$

in which narrow lobes appear at the multiples of the modulation frequency, $\omega_m = \pi/\tau$, with $c_k = \frac{1}{2\tau}\int_0^{2\tau} f(t)e^{ik\omega_m t}dt$. In the case of very short RF-pulses, $|c_{\pm k}|^2 = 4\sin(k\pi/2)^2/k^4\pi^2\omega_m^2$, which permits to neglect all lobes but the first one. With the inclusion of spin relaxation, the dominant spectral peak gives the echo peak amplitude

$$E(t) = \sum_i E_{oi} e^{-\frac{t}{T_{2i}} - \frac{8\gamma^2}{\pi^2\omega_m^2}\vec{G}_i.\underline{D}_i(\omega_m).\vec{G}_i t}. \quad (12)$$

in which MFG, $\gamma\vec{G}_i$, is the average of $\langle \nabla\omega_z(\vec{r}_i,t) \rangle$ over the spin trajectory during the time $t = N\tau$. Here, we assume that T_{2i} contains also possible diffusion/spin relaxation correlations. By changing the period, τ, we change the modulation frequency and trace out the frequency dependence of spectrum, according to Eq. (12) [27]. The sum over all individual spins can be grouped into separate sub-ensembles, in which the dynamical behavior may be different due to the pore size dispersion, which is given by the distribution of $\underline{D}_i(\omega_m)$, or due to differences of $\vec{G}_i$ observed by spin inside the pore. Namely, one might distinguish spins having a different starting point for their motion within a pore but the diffusion motion across the pore space averages MFG depending on the length of trajectory. For such grouping, the averages within different sub-ensembles have to be separately handled.

The MGSE method excels among others methods by allowing instant insight into different modes of molecular translational motion. In the case of restricted diffusion, the complete VAS contains information about all regimes of motion: About almost free diffusion at high frequencies, the restricted motion between enclosing boundaries at intermediate frequencies, and about the exchange between interconnected pores at very low frequencies.

Here, we demonstrate the ability of MGSE method to determine molecular dynamics in porous media without the externally applied MFG but only with the employment of MFG, which is generated by the magnetic susceptibility differences at solid/liquid interfaces and/or magnetic impurities.

2.3. VAS of molecular restricted self-diffusion

The velocity autocorrelation function of Brownian motion in the system of finite size can be obtained from the solution of Langevin equation [48] or from the second derivative of the mean squared displacement (MSD) calculated by using the probability distribution of the Fick's diffusion equation [46], which can be written for the diffusion within porous structure of an arbitrary geometry and a spin at the starting point $\vec{r}_o$ as

$$P(\vec{r},t|\vec{r}_o) = \sum_{\vec{k}} \psi(\vec{r})_{\vec{k}}\psi(\vec{r}_o)_{\vec{k}} e^{-t/\tau_{\vec{k}}}. \quad (13)$$

Here, $\tau_{\vec{k}}$ is the characteristic time of the $\vec{k}$-th diffusion mode and $\psi(\vec{r})_{\vec{k}}$ is its eigen function. The spin mean square displacement (MSD) along the direction of MFG at the location $\vec{r}$ in the pore [46] is given by

$$\langle \Delta R^2 \rangle(\vec{r},t,\vec{g}) = \int_V (\vec{g}(\vec{r}-\vec{r}_o))^2 P(\vec{r},t|\vec{r}_o)\, d\vec{r}_o, \quad (14)$$

in which $\vec{g}$ is the unit vector pointing along MFG. The Fourier transformation of MSD gives VAS of restricted diffusion as

$$-\omega^2 \int_0^\infty \langle \Delta R^2 \rangle(\vec{r},t,\vec{g}) \cos\omega t\, dt = \vec{g}\cdot\underline{D}(\omega,\vec{r})\cdot\vec{g} = \sum_{k\neq 0} \vec{g}\cdot\underline{b}_{\vec{k}}(\vec{r})\cdot\vec{g}\,\frac{\tau_{\vec{k}}\omega^2}{1+\tau_{\vec{k}}^2\omega^2}, \quad (15)$$

in which $\underline{b}_{\vec{k}}(\vec{r}) = \int_V (\vec{r}-\vec{r}_o)\otimes(\vec{r}-\vec{r}_o)\psi_{\vec{k}}(\vec{r}_o)\, d\vec{r}_o$ are termed the tensors of pore structure at location $\vec{r}$, because they depends on the pore geometry.

The restricted self-diffusion in a porous system is commonly divided in three regimes of motion: The almost free diffusion at short times with the diffusion displacement smaller than pore radius, an intermediate regime with the spin displacements comparable to the pore size, and the motional narrowing regime at long times, when spins repetitively cross the pore space. As shown in Ref. [32], $D(\omega)$ contains information about all three regimes: At high frequencies (short times), $D(\omega)$ levels to the value of the bulk diffusion coefficient, at the intermediate frequencies, $D(\omega)$ follows $\frac{1}{\sqrt{\omega}}$-dependence with the slope proportional to the surface-to-volume ratio of porous structure, $\frac{S}{V}$, while the low frequencies, the spectrum ω^2-dependence has the slope proportional to the fourth moment of pore diameters.

With substitution of Eq. (15) in Eq. (9), the attenuation of echo induced by the i-th spin is

$$\beta_i(t,\vec{r}) = \frac{t}{T_{2i}} + \frac{4\gamma^2}{\pi^2}\sum_{\vec{k}\neq 0} \vec{G}_i\underline{b}_{\vec{k}}(\vec{r}_i)\vec{G}_i \frac{\tau_{\vec{k}}\tau^2}{\tau^2+\pi^2\tau_{\vec{k}}^2} t. \quad (16)$$

Spins at different location within the pore space are subjected to the nonuniform magnetic susceptibility gradients, whose direction and magnitude vary within the space between the pore boundaries. Thus, the total echo signal consist of contributions induced by the spins, which are subjected to different MFG at different locations in a pore. According to the theory of statistics [49], the decay of

signal, which is the sum of many signals, whose decay rates, β_i, are randomly distributed, can be approximated by

$$\beta(t) \approx \log \sum_i e^{-\beta_i t} = -\langle\beta\rangle t + \frac{1}{2}\langle\beta^2\rangle t^2 - \frac{1}{6}\langle\beta^3\rangle t^2 \ldots \quad (17)$$

Here $\langle\beta\rangle$ is the mean decay rate, while $\langle\beta^n\rangle$ is the n-th central moment of β_i distribution respectively. Thus, $\langle\beta^2\rangle$ is the variance while $\langle\beta^3\rangle$ is related to the skewness of the decay distribution. In the case of the restricted diffusion in a poorly permeable pore, when $b_1\tau_1 \gg b_k\tau_k$ for $k > 1$ and with $\tau \geqslant \tau_1$, in which the first correlation time, τ_1, is about the duration of particle flight across pore space, the attenuation can be approximated by the first terms of $\vec{k}$ summation, as shown on Fig. 1. With these assumptions, the attenuation of spin echo at $t = 2N\tau > \tau_1$, can be approximated as

$$\beta(t)/t \approx \frac{1}{T_2} + \frac{4\gamma^2}{\pi^2} G^2 b_1 \frac{\tau_1\tau^2}{\tau^2 + \pi^2\tau_1^2} - \ldots \quad (18)$$

Here, we assume the spin trajectories long enough to cross the pore space several times and to permit an approximation $\langle \vec{G}_i)\underline{b}_1(\vec{r}_i)\vec{G}_i\rangle \approx G^2 b_1$, with G being the mean MFG and b_1 the mean pore structure parameter respectively. Minor differences in the form of VAS for pores of different geometries [32] permits to simplify the porous media with the system by spherical pores of diameter a with the structure parameter $b_1 = 0.25a^2$ [50]. Fig. 1 shows $\beta(\tau)/t$ calculated for the case of the diffusion in the spherical pore with the externally applied linear gradient field. At long τ, after the multiple passages between pore boundaries β/t levels to the value proportional to $b_1\tau_1 = 2\frac{\chi^4 a^4}{D}$, in which $\chi = 0.23$ [32]. The dependence of attenuation on the pore size is particularly visible at long τ, while at very short τ, at the proximity of intersection with the abscissa at $1/T_2$, it can be approximated as

$$\beta(\tau)/t \approx \frac{t}{T_2} + \frac{8\gamma^2 G^2\tau^2}{\pi^4} D_o\left(1 + c\frac{S}{3\sqrt{2}V}\sqrt{D_o\tau} + \ldots\right), \quad (19)$$

with D_o being the bulk diffusion coefficient, $\frac{S}{V}$ the surface to volume ratio and with c equal to $3, 3/2$ and 1 for plan-parallel, cylindrical and spherical pores respectively, but only when MFG is applied perpendicular to the walls of pore. While in the medium of the randomly distributed slabs or cylindrical pores the factor c equals to 1. Fig. 1 shows that the attenuation dependence on $\frac{S}{V}$ is observed below $\tau < \tau_1$.

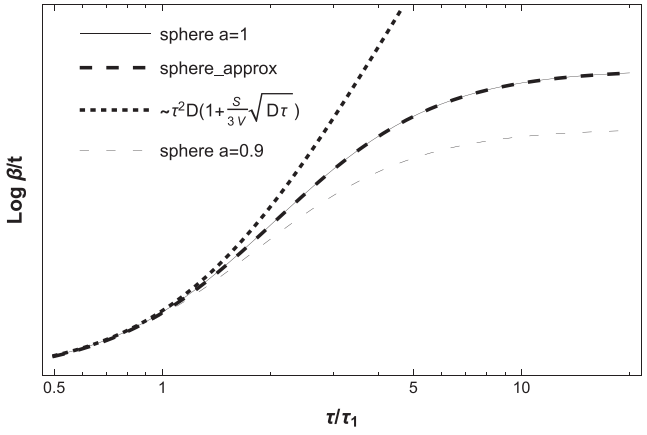

Fig. 1. The spin echo attenuation for the restricted diffusion in spherical pores, β/t versus τ/τ_1, calculated with Eq. (16) for the pore of radius $a = 1$ (thin curve) and $a = 0.9$ (thin doted curve). There are also the approximations with Eq. (18) (thick dotted curve), and the S/V dependence according to Eq. (19) (dotted curve).

3. Experiments

The cement pastes were prepared using a gray cement CEM I 52.5 R (Holcim, Romania). The cement contains 96.5% clinker and 3.4% auxiliary components (gypsum). The clinker is composed of C_3S (73%), C_2S (4%), C_3A (4%) and C_4AF (15.5%) with a relatively high amount of Fe_2O_3 (5%) as provided by the manufacturer. The samples were prepared at room temperature with a water-to-cement (w/c) ratio of 0.3 using distilled water produced in our laboratory. The mixture was homogenized for 6 min using an electric mixer with a rotational frequency of 500 rpm.

Immediately after mixing, the obtained samples were poured into NMR tubes with 10 mm external diameter, which fit inside a low field NMR instrument (Bruker MINISPEC MQ20,3 Bruker, Germany) operating at 20 MHz proton resonance frequency. The hydration process of all samples took place within the opened tube maintained inside the NMR sample unit at a controlled temperature of 23 °C and 35 °C respectively and a humidity of about 60%. To avoid the edge effects on our measurements we used bigger amount of sample, exceeding the active volume of RF coil. The first measurements were always performed at 15 min counting from the initiation of the mixing process and the last after 5 h of hydration.

The CPMG echo trains were recorded at different hydration times between 15 min and 5 h. The recording duration of a complete CPMG echo train experiment was shorter than 40 s which ensures no sample changes during the experiment. The CPMG series were recorded with increased inter pulse spacing between 0.1 ms and 0.4 ms respectively. The lower limit was set by the hardware limitations of our NMR instrument. The upper limit was determined by the fact that no more variation in the slope of the CPMG echo train could be detected.

4. Discussion

Tipical echo attenuations are shown in Figs. 2 and 3 for two different echo times (0.1 ms and 0.25 ms) and two different hydration times (0.25 h and 3 h). The curves exhibit an initial deviation from the exponential decay, which is particularly pronounced for decays at short τ. Here we explain it with the MFG differences inside the pore playing the role at short spin displacements. However, after a few milliseconds, corresponding to the time of many passages across the space of pore, the decay pass into an almost clear exponential one. It means that after an interval long enough, the attenuation is determined by the averaged MFG along the motional

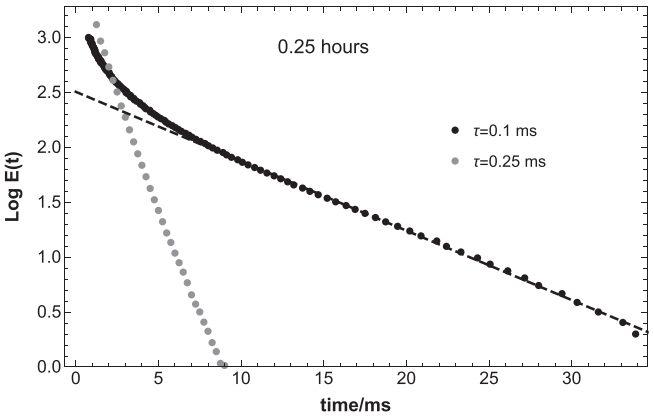

Fig. 2. The decay of spin echo amplitude for two different intervals between π-RF pulses, $\tau = 0.1$ and 0.25 ms, after 0.25 h of cement hydration at the temperature of 23 °C.

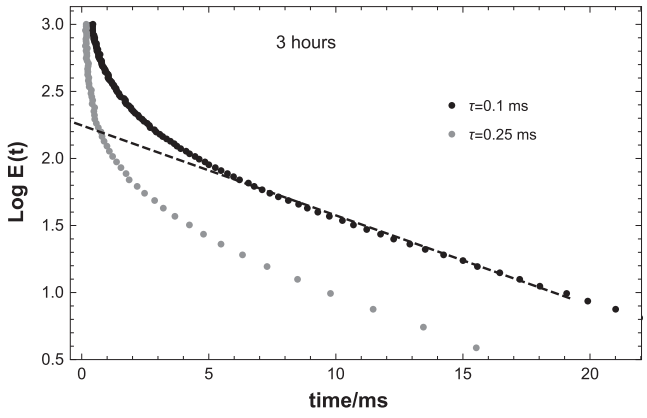

Fig. 3. The decay of spin echo amplitude for two different intervals between π-RF pulses, $\tau = 0.1$ and 0.25 ms, after 3 h of cement hydration at the temperature of 23 °C.

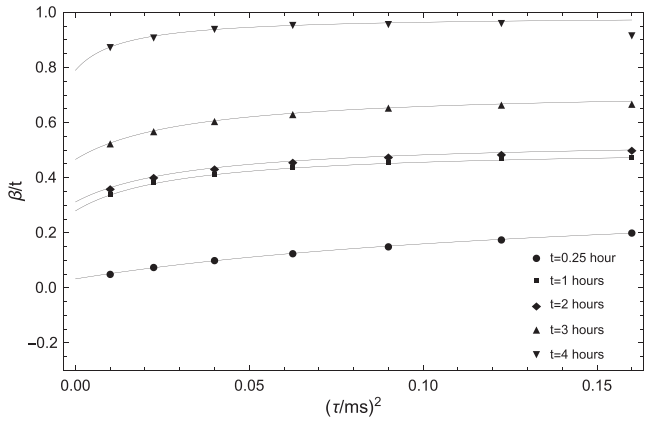

Fig. 5. The dependence of spin echo attenuation on the interval between the rf pulses at different stages of cement hydration at temperature 35 °C with the fitting curves according to Eq. (18).

trajectory of spin. By changing the inter pulse spacing τ from 0.1 to 0.4 ms, and by neglecting the initial non-exponential part of the decay, the slope of $\beta(t)$ gives the signal attenuation as a function of interval between the rf pulses. Figs. 4 and 5 show β/t versus τ^2, at different stages of cement hydration and at temperatures 23 °C and 35 °C respectively. The added curves represent the fit of Eq. (18) to the experimental data. Except for very long times of cement hydration, the curves adapt well with the experimental points that confirms the assumption about the spin echo attenuation that is caused by the diffusion of water in the internal MFG induced by the susceptibility differences at the liquid-solid interfaces of capillary pores inside cement paste. The fitting parameters shows how the spin relaxation, the mean size of capillary pores and the mean MFG are changing with the hydration process at different temperatures as shown on Figs. 6–8 respectively.

While the spin relaxation exhibits the expected dependence on the time of hydration and temperature, as shown on Fig. 6, the obtained sizes of pores are in the range observed by the electronic microscopy of hardened cement paste and in the same range with those reported in Ref. [2] for similar samples but under conditions of full hydration. However, the advantage of the MGSE method is that it can monitors changes during induction period and early acceleratory stage of hydration. An increase in the gradient strength by reducing the pore size during the process of hydration, shown on Figs. 7 and 8, confirms the assumption about an averaged magnitude of MFG observed by spin after it trajectory is

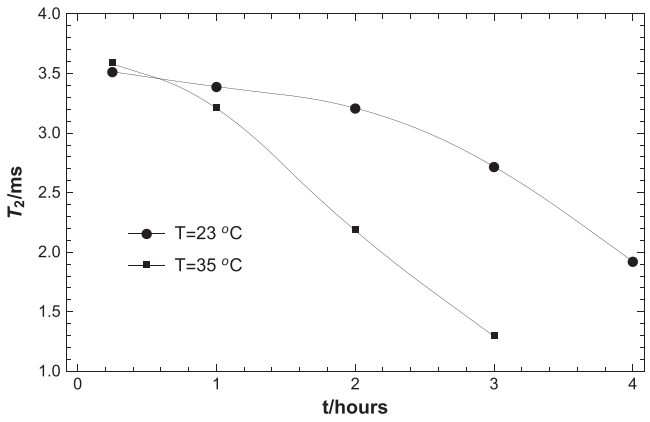

Fig. 6. The spin relaxation dependence on time of hydration as obtained from the data fit with Eq. (18).

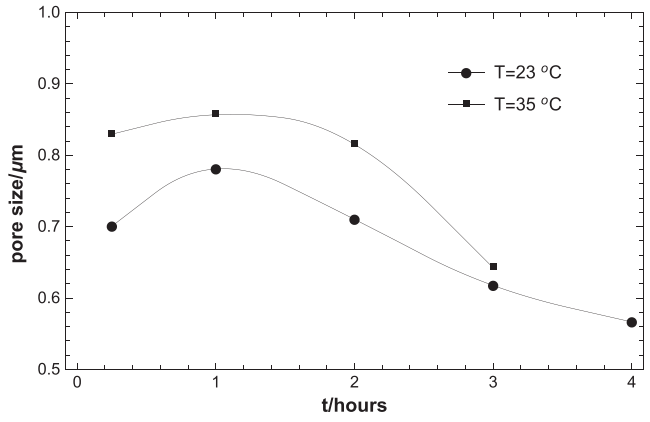

Fig. 7. The mean size of capillary pores at early stages of hydration process as obtained from the fit of Eq. (18) to the experimental data with the assumption of nearly spherical pores.

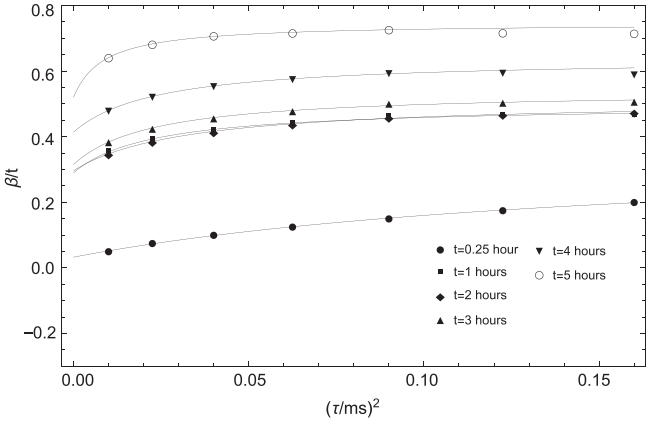

Fig. 4. The dependence of the signal attenuation on the interval between the rf pulses at different stages of cement hydration at temperature 23 °C with the fitting curves according to Eq. (18).

repeatedly crossing the pore space during the time intervals, which are larger than τ_1. Namely, the pore size reduction increases the number of flights in the proximity of area with the strong MFG at solid/liquid interfaces. However, it is not the case for the decay at short times, which shows a pronounced non-exponentiality, particularly at short modulation times, τ. We explain it with the distribution of relaxation times that appears at the displacements

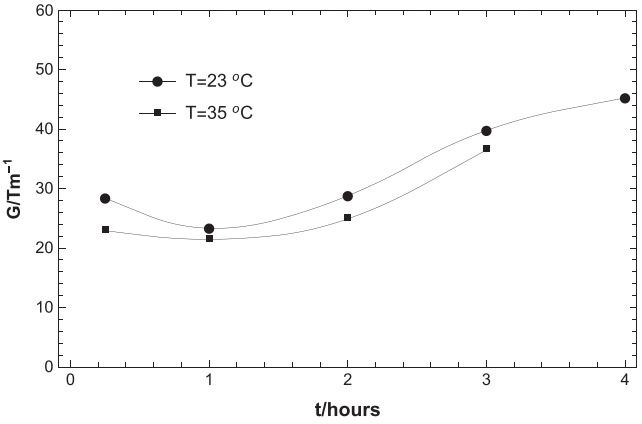

Fig. 8. Averaged internal magnetic field gradient at different stages of hydration as obtained from the fit of Eq. (18) to experimental data.

short enough that spin may observe the differences of MFG within the pore space. The expansion of spin echo decay, $\log E(t)/E(0)$, into the Taylor series provides the mean and the variance of the relaxation time distribution and thereby also the distribution of MFG. The analysis of initial decays in the interval to about 10 μs, shown on Figs. 2 and 3 for $\tau = 0.1$ μs, gives the peak of MFG distribution, which is 6 times larger than values shown on Fig. 8, while the obtained variance is about 60% its peak value. Thus, the estimated maximal gradient at the solid-liquid interfaces could be about 200 T/m. The attenuation dependence on the pore size appears very visible at long intervals τ, as shown on Fig. 1. Thus, the non-exponential deviations at long decay times, shown on Fig. 2 for $\tau = 0.25$ ms after 0.25 h of hydration and on Fig. 3 for $\tau = 0.25$ after 3 h of hydration, belong to the pore size dispersion. The second time derivative of the attenuation time dependence provides the variance of the pore size distribution, which is about 15% of the pore mean size after 0.25 h and about 55% after 3 h of hydration at the temperature of 23 °C.

5. Conclusion

After many years of research, porous media, which are ubiquitous in modern life, from natural materials such as rocks, wood, and packed snow, to man-made materials such as concretes and food products, and to biologic tissues such as bones and lungs, remains a challenge due to the complexity of their internal structure and the molecular dynamic of confined liquid. Although, the internal susceptibility-induced magnetic field are commonly considered, as an inevitable obstacle at the diffusion measurements in porous media by PGSE methods, we demonstrate the ability of MGSE method to employ these fields to provide relevant information about the time evolution of capillary pores of cement materials. The theoretical treatment discussed here gives a better understanding of spin interaction with the radio-frequency in the presence of the non-uniform magnetic field, which may remove the fear that has so far constrained the full use of CPMG sequence for diffusion measurements, particularly in the presence of a very inhomogeneous susceptibility induced magnetic fields in porous media.

Acknowledgement

I.A. acknowledges the Romanian National Authority for Scientific Research (CNCS UEFISCDI) for a grant PN-II-ID-PCE-2011-3-0238 and J. S. is grateful to the Slovenian Research Agency for the financial support within the frame of the National Research and Development Programs.

References

[1] S. Kosmatka, B. Kerkhoff, W. Panarese, Design and Control of Concrete Mixtures, vol. 14, EB001, Portland Cement Association, Skokie, Illinois, USA, 2003, pp. 2–5, doi: 2001007603
[2] J. Korb, L. Monteilhet, P. McDonald, J. Mitchell, Microstructure and texture of hydrated cement - based materials: a proton field cycling relaxometry approach, Cem. Concr. Res. 37 (2007) 295–302, http://dx.doi.org/10.1016/j.cemconres.2006.08.002.
[3] P. McDonald, V. Rodin, A. Valori, Characterisation of intra - and inter -C-S-H gel pore water in white cement based on an analysis of NMR signal amplitudes as a function of water content, Cem. Concr. Res. 40 (12) (2010) 1656–1663, http://dx.doi.org/10.1016/j.cemconres.2010.08.003.
[4] A. Muller, K. Scrivener, A. Gajewicz, P. McDonald, Densification of C-S-H measured by ^{1}H NMR relaxometry, J. Phys. Chem. C 117 (2012) 403–412, http://dx.doi.org/10.1021/jp3102964.
[5] H. Chengyi, R. Feldman, Influence of silica fume on the micro - structural development in cement mortars, Cem. Concr. Res. 15 (1985) 285–294, http://dx.doi.org/10.1016/0008 - 8846(85)90040 - 7.
[6] A. Pop, C. Badea, I. Ardelean, The effects of different super - plasticizers and water - to - cement ratios on the hydration of gray cement using T_2 - NMR, Appl. Magn. Reson. 44 (2013) 1223–1234, http://dx.doi.org/10.1007/s00723 - 013 - 0475 - 5.
[7] A. Pop, A. Bede, M. Dudescu, F. Popa, I. Ardelean, Monitoring the influence of aminosilane on cement hydration via low - field NMR relaxometry, Appl. Magn. Reson. 47 (2015) 191–199, http://dx.doi.org/10.1007/s00723 - 015 - 0743 - 7.
[8] A. Bede, A. Pop, M. Moldovan, I. Ardelean, The influence of silanized nano - SiO_2 on the hydration of cement paste: NMR investigations, AIP Conf. Proc., 17, 2015, p. 60009, doi:0.
[9] C. Badea, A. Pop, C. Mattea, S. Stapf, I. Ardelean, The effect of curing temperature on early hydration of gray cement via fast field cycling - NMR relaxometry, Appl. Magn. Reson. 45 (2014) 1299–1309, http://dx.doi.org/10.1007/s00723 - 014 - 0565 - z.
[10] M. Hoseini, V. Bindiganavile, N. Banthia, The effect of mechanical stress on permeability of concrete: a review, Cem. Concr. Compos. 31 (2009) 213–220, http://dx.doi.org/10.1016/j.cemconcomp.2009.02.003.
[11] R.M.E. Valckenborg, L. Pel, K. Hazrati, K. Kopinga, Pore water distribution in mortar during drying as determined by NMR, Mater. Struct. 34 (2001) 599–604.
[12] F. Barberon, P. Korb, D. Petit, V. Morin, E. Bermejo, Probing the surface area of a cement - based material by nuclear magnetic relaxation dispersion, Phys. Rev. Lett. 90 (2003) 116103, http://dx.doi.org/10.1103/PhysRevLett.90.116103.
[13] S. Diamond, Mercury porosimetry: an inappropriate method for the measurement of pore size distributions in cement - based materials, Cem. Concr. Res. 30 (2000) 1517–1525.
[14] G. Padhy, C. Lemaire, E. Amirtharaj, M.A. Ioannidis, Pore size distribution in multiscale porous media as revealed by DDIF - NMR, mercury porosimetry and statistical image analysis, Colloids Surfaces A Physicochem. Eng. Asp. 300 (2007) 222–234, http://dx.doi.org/10.1016/j.colsurfa.2006.12.039.
[15] I. Ardelean, R. Kimmich, Principles and unconventional aspects of NMR diffusometry, Annu. Reports NMR Spectrosc. 49 (2003) 43–115.
[16] N. Nestle, P. Galvosas, J. Kärger, Liquid - phase self - diffusion in hydrating cement pastes - results from NMR studies and perspectives for further research, Cem. Concr. Res. 37 (2007) 398–413, http://dx.doi.org/10.1016/j.cemconres.2006.02.004.
[17] M. Hürlimann, Effective gradients in porous media due to susceptibility differences, J. Mag. Res 131 (1998) 232–240, http://dx.doi.org/10.1006/jmre.1998.1364.
[18] L. Zielinski, Effect of internal gradients in the nuclear magnetic resonance measurement of the surface - to - volume ratio, J. Chem. Phys. 121 (2004) 352–361, http://dx.doi.org/10.1063/1.1756873.
[19] Y.-Q. Song, Using internal magnetic fields to obtain pore size distributions of porous media, Concepts Magn. Reson. 18A (2003) 97–110, http://dx.doi.org/10.1002/cmr.a.10072.
[20] S. Muncaci, I. Ardelean, Probing the pore size of porous ceramics with controlled amount of magnetic impurities via diffusion effects on the CPMG technique, Appl. Magn. Reson. 44 (2013) 837–848, http://dx.doi.org/10.1007/s00723 - 013 - 0454 - x.
[21] A. Pop, I. Ardelean, Monitoring the size evolution of capillary pores in cement paste during the early hydration via diffusion in internal gradients, Cem. Concr. Res. 77 (2015) 76–81, http://dx.doi.org/10.1016/j.cemconres.2015.07.004.
[22] J. Stepišnik, P. Callaghan, The long time-tail of molecular velocity correlation in a confined fluid: observation by modulated gradient spin echo NMR, Physica B 292 (2000) 296–301.
[23] P. Callaghan, J. Stepišnik, in: Warren S. Warren (Ed.), Advances in Magnetic and Optical Resonance, vol. 19, Academic Press, Inc, San Diego, 1996, pp. 326–389 (Chapter Generalised Analysis of Motion Using Magnetic Field Gradients).
[24] H.Y. Carr, E.M. Purcell, Effects of diffusion on free precession in nuclear magnetic resonance, Phys. Rev. 94 (1954) 630–638.
[25] S. Meiboom, D. Gill, Modified spin-echo method for measuring nuclear relaxation times, Rev. Sci. Inst. 29 (1958) 688–691.
[26] J. Stepišnik, Analysis of NMR self-diffusion measurements by density matrix calculation, Physica B 104 (1981) 350–364.

[27] P. Callaghan, J. Stepišnik, Frequency-domain analysis of spin motion using modulated gradient NMR, J. Magn. Reson. A 117 (1995) 118–122.
[28] P.T. Callaghan, S.L. Codd, Flow coherence in a bead pack observed using frequency domain modulated gradient nuclear magnetic resonance, Phys. Fluids 13 (2001) 421–426.
[29] D. Topgaard, C. Malmborg, O. Soederman, Restricted self-diffusion of water in a highly concentrated w/o emulsion studied using modulated gradient spin-echo NMR, J. Mag. Res. 156 (2002) 195–201.
[30] E.C. Parsons, M.D. Does, J.C. Gore, Modified oscillating gradient pulses for direct sampling of the diffusion spectrum suitable for imaging sequences, Magn. Reson. Imaging 21 (2003) 279–285.
[31] S. Lasič, J. Stepišnik, A. Mohorič, I. Serša, G. Planinšič, Autocorrelation spectra of an air-fluidized granular system measured by NMR, Europhys. Lett. 75 (2006) 887–893.
[32] J. Stepišnik, S. Lasič, A. Mohorič, I. Serša, A. Sepe, Spectral characterization of diffusion in porous media by the modulated gradient spin echo with CPMG sequence, J. Magn. Reson. 182 (2006) 195–199.
[33] R.P. Feynman, An operator calculus having applications in quantum electrodynamics, Phys. Rev. 84 (1951) 109–128.
[34] F. Dyson, The radiation theories of Tomonaga, Schwinger, and Feynman, Phys. Rev. 75 (1949) 486.
[35] M.D. Hürlimann, D.D. Griffin, Spin dynamics of Carr - Purcell -Meiboom - Gill-like sequences in grossly inhomogeneous B_0 and B_1 fields and application to NMR well logging, J. Magn. Reson. 143 (2000) 120–135.
[36] M.D. Hürlimann, Diffusion and relaxation effects in general stray field NMR experiments, J. Magn. Reson. 148 (2001) 367–378.
[37] Y.Q. Song, Categories of coherence pathways for the CPMG sequence, J. Magn. Reson. 157 (2002) 82–91.
[38] E. Toumelin, C. Torres-Verdn, B. Sun, K. Dunn, Random-walk technique for simulating NMR measurements and 2d NMR maps of porous media with relaxing and permeable boundaries, J. Magn. Reson. 188 (2007) 83–96.
[39] I. Serša, F. Bajd, A. Mohorič, Effects of off-resonance spins on the performance of the modulated gradient spin echo sequence, J. Magn. Reson. 270 (2016) 77–86.
[40] E.O. Stejskal, J.E. Tanner, Spin diffusion measurements: spin-echoes in the presence of a time-dependent field gradient, J. Chem. Phys. 42 (1965) 288–292.
[41] W. Magnus, On the exponential solution of differential equations for a linear operator, Commun. Pure Appl. Math. 7 (1954) 649–673.
[42] J. Stepišnik, I. Ardelean, Exploiting the internal magnetic susceptibility gradient for the characterization of porous materials by using MGSE method, in: S. Jurga, (Ed.), AMPERE Summer school, Zakopane, 2016.
[43] J. Stepišnik, Measurement of molecular dynamics in liquids by NMR CPMG method: revisited (submitted for publication).
[44] J. Stepišnik, A. Mohorič, C. Matea, S. Stapf, I. Serša, Velocity autocorrelation spectra in molten polymer measured by NMR modulated gradient spin-echo, EuroPhysics Lett. 106 (2014), http://dx.doi.org/10.1209/0295-5075/106/27007, 270–07.
[45] A. Mohorič, J. Stepišnik, NMR in the earth's magnetic field, Prog. Nucl. Magn. Reson. Spectrosc. 54 (2009) 166–182.
[46] J. Stepišnik, A new view of the spin echo diffusive diffraction in porous structures, Europhysics Lett. 60 (2002) 453–459.
[47] J. Stepišnik, Measuring and imaging of flow by NMR, Prog. Nucl. Magn. Reson. Spectrosc. 17 (1985) 187–209.
[48] E. Oppenheim, P. Mazur, Brownian motion in system of finite size, Physica 30 (1964) 1833–1845.
[49] R. Kubo, Some Aspects of the Statistical-Mechanical Theory of Irreversible Processes in 'Lectures on Theoretical Physics', Interscience Publisher, 1959.
[50] J. Stepišnik, Time dependent self-diffusion by NMR spin-echo, Physica B 183 (1993) 343–350.